Chapter I

Magneto-optical study of Cr-doped CdTe quantum dots

In this chapter, we will study the photoluminescence of a single Chromium atom in a II-VI quantum dot. We saw in the chapter I that the magnetic anisotropy of the spin lead to a zero magnetic field splitting of the 0, ± 1 and ± 2 states. In a neutral Cr-doped quantum dot, such a magnetic anisotropy is induced by the bi-axial strain in the plane of the dots. Studying the magnetic-field dependence of the quantum dots photoluminescence, we will also show the influence of the quantum dot symmetry on carrier-Cr spin coupling. The proximity of dark lead to a characteristic repartition of intensity on the three luminescence peak of the QD. However, some dots are not explained by this model, and need to take the position of Cr atom in regard of the dot into account.

I.1 A system strongly coupled to strain state at the Cr position

I.1.1 Energy structure of a Cr in a quantum dot

Using the procedure described in the second chapter, we randomly incorporated Cr atom in a CdTe/ZnTe quantum dots, adjusting the density of the Cr atoms to be roughly equal to the density of dots, in order to get QDs containing 0, 1 or a few Cr atoms. The emission of individual QDs, induced by optical excitation with a dye laser tuned on resonance with an excited state of the dots, is studied in magnetic fields (up to 11 T) by optical micro-spectroscopy in Faraday configuration [1].

The low temperature (T=5K) PL of the neutral exciton (X-Cr) and biexciton (X^2-Cr) of an individual Cr-doped QD are reported in Fig. I.1(b). Four emission lines are observed for the neutral species (X and X^2). Scanning with an energy

Figure I.1: Dot334 QD4 PLE with highlight on quasi-resonant state, and spectra X and X2, along X-X2 of dot334 QD3.

tunable laser, we saw that all this complex share a common quasi-resonant state, where all these peaks are at a maximum intensity, as highlighted in Fig. I.1(a). This is an indication that they originate from the same dot.

The relative intensities of the lines and their splitting change from dot to dot as illustrated in Fig. I.1 (b-c). A splitting of the central line is observed for X-Cr and X^2-Cr and an additional line appears on the low energy side of the X-Cr spectra. All these features result from the exchange coupling of the electron and hole spins with a single Cr spin.

One can observe a dependence of the quantum dot emission in linear polarization, presented in Fig. I.2. The central line (S_z=0) is split and linearly polarized along two orthogonal directions. As in non-magnetic QD, this results from a coupling of the two bright excitons $|\pm1\rangle$ by (i) the short range e-h exchange interaction in the presence of valence band mixing and/or (ii) the long-range e-h exchange interaction in a QD with an in-plane shape anisotropy [2]. This anisotropic e-h exchange energy mixes the bright exciton associated with the same Cr spin state, inducing an extra splitting between them. The mixing is maximum for the central pair of bright exciton (S_z=0) which are initially degenerated. The outer lines are also slightly linearly polarized but the influence of the e-h exchange interaction is attenuated by the initial splitting of the $|\pm1\rangle$ excitons induced by the exchange interaction with the Cr spin S_z=±1.

Looking at the time resolved photoluminescence, presented in Fig. I.3, we see that the line (4) present a decay time about twice as long as the high energy peak. A long recombination time one of the characteristic of a dark exciton emission [3].

2

Figure I.2: Graph in π_x and π_y above linear polarization of dot338 QD3

Figure I.3: Decay time on dot338 QD3

Under normal circumstances, a dark exciton recombination is non-radiative. However, it possible to observe a dark exciton recombination emitting a photon in low symmetry quantum dot [4]. This hypothesis will be confirmed by the magneto-optical study of the dot presented in Fig. I.7 and I.8.

In a II-VI semiconductor, the orbital momentum of the Cr connects the spin of the atom to its local strain environment through the modification of the crystal field and the spin-orbit coupling. For biaxial strain in the (001) plane, the ground state of a Cr spin is split by a strain induced magnetic anisotropy term $\mathcal{H}_{Cr,\varepsilon_\parallel} =$

Figure I.4: Overall energy structure (with +/- 2 with no luminescence)

$D_0 S_z^2$ (see chap. I). It was deduced from electron paramagnetic resonance of bulk Cr-doped CdTe that D_0 is positive for compressive biaxial strain [5]. In a self-assembled CdTe/ZnTe QD with large in-plane strain, the Cr spin energy levels are split with S_z=0 at low energy (Fig. I.4). A value of D_0 in the 1 meV range can be expected for a CdTe layer strained on a ZnTe substrate, as shown in chap.I.

When an electron-hole (e-h) pair is injected in a Cr-doped QD, the bright excitons are split by the exchange interaction between the spins of Cr and carriers. In flat self-assembled QDs, the heavy-holes and light-holes are separated in energy by the biaxial strain and the confinement. In a first approximation, the ground state in such QD is a pure heavy-hole (J_z=$\pm 3/2$) exciton and the exchange interaction with the Cr spin S is described by the spin Hamiltonian $\mathcal{H}_{c-Cr} = I_{eCr}\vec{S}\cdot\vec{\sigma} + I_{hCr}S_z J_z$, with $\vec{\sigma}$ the electron spin and J_z the hole spin operator. I_{eCr} and I_{hCr} are, respectively, the exchange integrals of the electron and the hole spins with the Cr spin. These exchange energies depend on the exchange constant of the $3d$ electrons of the Cr with the carriers in CdTe and on the overlap of the Cr atom with the confined carriers. The exchange interaction of the Cr spin is ferromagnetic for both electron and hole spins in common II-VI semiconductors and a typical exchange constant 4 to 5 times larger for the holes than for the electrons is also expected in CdTe [6, 7].

For highly strained CdTe/ZnTe QDs with a weak hole confinement, the strain induced energy splitting of the Cr spin $D_0 S_z^2$ is much larger than the exchange energy with the confined carriers ($D_0 \gg |I_{hCr}| > |I_{eCr}|$). The exchange interaction with the exciton acts as an effective magnetic field which further splits the Cr spins states S_z=± 1 and S_z=± 2. The resulting X-Cr energy levels are presented

Figure I.5: dot338 QD3 spectra temperature evolution

in Fig. I.4. The exciton recombination does not affect the Cr atom and its spin is conserved during the optical transitions. Consequently, the large strained induced splitting of the Cr spin is not directly observed in the optical spectra. However, at low temperature, the Cr spin thermalize on the low energy states S_z=0 and S_z=$\pm$1. This leads to a PL dominated by three contributions: A central line corresponding to S_z=0 and the two outer lines associated with S_z=$\pm$1 split by the exchange interaction with the carriers.

Since the thermal energy do not allow the $\pm$2 level to be populated, we tried to rise the sample temperature and see if we were able to have emission corresponding to them. The results of this experiment are presented in Fig. I.5. We were able to go to 40K before the peak broadening and the interaction with phonon completely blurred the quantum dot emission. However, even at those temperatures, no emission of the $\pm$2 level was observed.

The scan map itself present some other point of interest, highlighted in Fig. I.6.

The first remarkable feature of this scan is the really long luminescence of the acoustic phonon replica. As shown on the zoom in Fig. I.6 [FIG LETTER HERE], the peaks still emit with an excitation several meV above the line and the dot emission energy, going until 2004 meV. One can also see to sharp intensity diminution in this emission. Mapping the intensity of this peak emission to the quantum dot spectrum, it is evidenced that these diminution occur when the laser is in resonance with a QD emission line. The absorption the preferentially occur in this resonantly excited state than in the acoustic phonon band.

Scanning the dot from close, one can see that it present several excited state.

Figure I.6: PLE of dot338 QD3. Highlight on different interesting part (mail 17/02/07 – 21:12).

The first one to appear, the one at lower energy, is around 2018.5 meV. On this excited, each peaks as a slightly different resonant energy. One can see that the order of appearance of the two central peaks seems to be reversed compared to the external ones. This phenomenon was first observed on QDs in GaAs quantum well [8]. This indicate an inversion of the splitting due to electron-hole exchange interaction [2].

Another excited state can be saw at 2025 meV. This excited state is also really large and can be linked back to an excitation to the optical phonon. Looking at the σ polarized emission of this state (Fig. I.6 [FIG LETTER HERE]), we can see that this excitation present a really good spin conservation: as can be seen on the emission on a dot quasi-resonant state, the low and high energy peak are strongly σ polarized, while the central peaks do not show dependency other circular polarization.

Finally, a last interesting excited state appear at 2030 meV. This state present an exchange-induced splitting different from the splitting in the quasi-resonant state. This is due to a difference in the carriers and Cr atom wavefunction overlap. One can also noticed the this state present a stronger luminescence in σ_{cross} than in σ_{co}: [TO REDISCUSS] this indicate a spin flip of the hole before the recombination.

I.1.2 Deduction of the quantum dot parameters

The structure of the energy levels in Cr-doped QDs is confirmed by the evolution of the PL spectra in magnetic field, presented in Fig. I.7. One can see that the

Figure I.7: Magneto-optic of dot334 QD3 and dot334 QD4 (X + X2)

Zeeman energy of the exciton under magnetic field can compensate the exciton splitting induced by the exchange interaction with the Cr [9]. For QD3, this results in an anti-crossing of $|+1\rangle$ and $|-1\rangle$ excitons due to the e-h exchange interaction around B_z=6 T observed both in $\sigma+$ and σ- polarizations (anti-crossing (2) and (3) in Fig. I.7(a)).

The low energy emission presented as a dark exciton in Fig. I.3 show an anti-crossing with the bright excitons under B_z in σ- polarization (anti-crossing (4) in Fig. I.7). As illustrated in Fig. I.8(c) this anti-crossing arises from a mixing of the bright and dark excitons interacting with the same Cr spin state. Observed in σ-polarization, it corresponds to the mixing of the exciton states $|-1\rangle$ and $|+2\rangle$ coupled to the Cr spin S_z=-1. This dark/bright exciton coupling δ_{12} is induced by the e-h exchange interaction in a confining potential of reduced symmetry (lower than C_{2v}) [10]. In such symmetry, the dark excitons acquire an in-plane dipole moment which lead to possible optical recombination at zero magnetic field [4] as observed in these QDs. The oscillator strength of this "dark exciton" increases as the initial splitting between $|-1\rangle$ and $|+2\rangle$ excitons is reduced by the magnetic field (Fig. I.8(c)).

To illustrate the influence of the QD symmetry on the magneto-optical properties of X-Cr, we compare in Fig. I.7 the emission of two QDs with different strain state, QD1 in (a) and QD2 in (b). For QD1, the splitting of the central peak is not clear in the PL at 0T (Fig. I.1(a)) without the linear polarization map, while two linearly polarized peaks appears clearly in QD2 spectra. This difference in emission arise from a difference in the in-plane strain of each QD [2]. The dark exciton emission is also stronger in QD2, confirming a lower symmetry than QD1.

7

Investigating both the biexciton and the exciton in the same Cr-doped QD, we can also analyze the impact of the carrier-Cr interaction on the fine structure of the Cr spin. The magnetic field dependence of X^2-Cr and X-Cr emissions in QD4 are presented as a contour plot in Fig. I.7(b) and (c) respectively. The PL under magnetic field of X-Cr and X^2-Cr present a mirror symmetry. In particular, the dark/bright exciton mixing observed around B_z=2.5T on the low energy side of the PL in $\sigma-$ polarization for X-Cr is observed on the high energy side in $\sigma+$ polarization for X^2-Cr (circles in Fig. I.7(b) and (c)).

If one consider the ground state of X^2 as a spin-singlet (total spin 0), it cannot be split by the magnetic field or the spin interaction part of the carriers-Cr Hamiltonian. The creation of two excitons in the QD cancels the exchange interaction with the Cr atom. Thus, the PL of X^2-Cr is controlled by the final state of the optical transitions, i.e. the eigenstates of X-Cr, resulting in the observed mirror symmetry in the PL spectra. However, in some of the QDs, the X^2-Cr emission slightly deviates from this simple picture: a smaller energy splitting is observed for X^2-Cr compared to X-Cr (see X-Cr and X^2-Cr in Fig. I.1 and Fig. I.7). This shows that there is an interaction of X^2 with the Cr atom. It could result from a perturbation of the carriers' wave function by the interaction with the magnetic atom [11, 12] or a modification the local electric field which controls the Cr fine structure. Further investigations are required to explain this effect that goes beyond the purpose of this article.

Figure I.8: Linear PL + magneto-optics with modelisation and explanation of anti-crossing

We calculated the magneto-optic behaviour of Cr-doped QDs by diagonalizing the complete Hamiltonian of the e-h-Cr system presented in Chap. I. We considered

Table I.1: Values of the parameters used in the model of Cr-doped CdTe/ZnTe quantum dot presented in Fig. I.1(b). The value of the parameters not listed in the table is 0. The chosen values are typical for CdTe/ZnTe quantum dots and can be compared with parameters extracted from Mn-doped quantum dots [13, 14].

I_{eCr}	I_{hCr}	δ_0	δ_1	δ_{12}	δ_{11}	$\frac{\delta_{xz}}{\Delta_{lh}}$	$\frac{\delta_{xx,yy}}{\Delta_{lh}}$	D_0	g_{Cr}	g_e
μeV	μeV	meV	μeV	μeV	μeV			meV		
2	-0.7	-70	-280	-1	250	150	50	0.05	0.05	2.5

g_h	γ	η	T_{eff}
	$\mu eV/T^2$	μeV	K
0.4	1.5	25	25

the general case of QDs with a symmetry lower than C_{2v} (truncated ellipsoidal lens for instance [10]), and took into account the influence of this reduced symmetry on the valence band and on the e-h exchange interaction. The population of the X-Cr spin states split by the large magnetic anisotropy and the carriers-Cr exchange interaction is described by a spin effective temperature T_{eff}. The results of the model obtained with T_{eff}=25K, D_0=2.5 meV and an electron-Cr (hole-Cr) exchange interaction I_{eCr}=-70μeV (I_{hCr}=-280 μeV) are reported in Fig. I.8 (parameters not specific to Cr-doped QDs are listed in Tab. I.1). The PL of X-Cr at zero field and its evolution in magnetic field can be qualitatively reproduced. In particular, the description of the spin states occupation by T_{eff} is sufficient to reproduce the observed emission from the three low energy X-Cr levels (Cr spin states S_z=0 and S_z=±1). The splitting of the central line at zero field (anti-crossing (1)) and the anti-crossings under magnetic field (anti-crossings (2) and (3) around B_z=6T for the Cr spin states S_z=+1 and anti-crossings (4) with the dark exciton around B_z=2T) are also well reproduced by the model.

The magnetic anisotropy D_0 cannot be precisely extracted from the PL spectra. However, a too large value would produce a smaller PL intensity of the sates S_z=±1 than observed experimentally. In addition, for $D_0 < 2.25$ meV, an anti-crossing due to an electron-Cr flip-flop controlled by I_{eCr}, labelled (5) in Fig. I.8(c), would appear below B_z=11T on the central line in σ+ polarization.

Another source of informations on the system is its evolution under excitation power. Such an experiment is reported on Fig. I.9 (a). As expected, the PL is becoming more intense with the augmentation of the excitation laser, since more exciton are produced and thus injected in the quantum dot. However, this power augmentation response is not the same for each of the peaks. The two central peaks, associated with the $|0\rangle$ states, start with about twice the intensity of the $|\pm$

Figure I.9: Excitation power variations on dot334 QD3 and plot of the intensity of each peak

$1\rangle$ peaks for the most intense one, seemingly never reaching their maximum under our power range. However, when lowering the excitation power, they diminish quickly, and even seems to disappear at low energy, when exterior peaks still show luminescence. Plotting this evolution show that the two central peaks shows a super-linear evolution. On the other side, the exterior peaks begin by rising in intensity before diminishing in a sub-linear fashion. This is coherent with the usual picture, with high power populating preferentially X^2-Cr states, while low power populate preferentially X-Cr states [?]. Finally, one can notice that the dark exciton exhibit the same behaviour, but the maximum emission intensity is at slightly lower power than the $|\pm 1\rangle$.

The results of this evolution are well reproduced by our spin effective Hamiltonian, using the parameters found for the dot from the magneto-optics and the linear polarization fitting. The model results are presented in Fig. I.10. [NOT SURE, TO BE REDISCUSSED]The super-linear behaviour of the central peaks can be explained by the proximity of dark exciton states. High power excitation can unlock radiative recombination path to states remaining nonradiative at low excitation power [15]. Such states linked to the $|0\rangle$ state make the emission on its peaks present a super-linear behaviour when excited at high power.

One characteristic emerging from our model is the necessity to have a E value close to 0μeV to reproduce the measures. Now that we show that our model reproduce well the evolution of the emission under various type of excitation, we can run it to see the influence of E on the emission. Results of such a study are presented on Fig. I.11, (a) and (b) for the X-Cr system, and (c) and (d) for the

Figure I.10: Power variation simulation

Figure I.11: Linear polar and magneto-optics simulation with high E

X^e-Cr one. This simulation was done by applying a small magnetic anisotropy along the X axis of the quantum dot ($D_x = 50\mu$eV, $D_y = 0\mu$eV, to be compared with $D_z = 2500\mu$eV), creating an effective E from this strain anisotropy in the QD plane.

The first remarkable feature appear on the linear polarization dependency of the X-Cr system(Fig. I.11 (a)). While, with a small value of E, only the $|0\rangle$ states presented linear polarization, at higher value, $|\pm 1\rangle$ states also present some. The quantum dot should then appear to present six peaks when probed in circular

polarization. As expected, even with this high E vale, X^c-Cr doesn't present any linear polarization dependency, as shown on Fig. I.11 (c), and would in this case still present the usual three peaks structure.

The evolution of the emission under magnetic field also present different characteristic than a QD with magnetic anisotropy purely along z. Fig. I.11 (b) present the evolution in B of the X-Cr emission. Firstly, one can see anti-crossings at $\pm 5T$ appearing on both $|+1\rangle$ and $|-1\rangle$, and not only one of them. Moreover, around 0T, several anti-crossing appear, not only on the $|0\rangle$ peak, but also on the $|\pm 1\rangle$. X^c-Cr also present a peculiar magnetic field evolution in a QD with a E value, presented in Fig. I.11 (d). If, for high B, no anti-crossing is visible, one occur around 0T. This anti-crossing occur when the Zeeman effect of the Cr atom compensate the electron-Chromium interaction and the hole-Chromium interaction. Such an anti-crossing is characteristic of this type of dots and will be useful in their identification: while the six peaks of the X-Cr might be undistinguishable at 0T, X^c-Cr would still present 3 peaks and show this particular evolution under magnetic field.

I.2   The case of six peaks dots

We showed in the section I.1.2 that each emission can be doubled for a QD with a a non-null in-plane anisotropy, each of these peaks having dependency in linear polarization. Some dots present this structure, but their evolution in magnetic field didn't show any anti-crossing. Such a dot is presented in Fig. I.12.
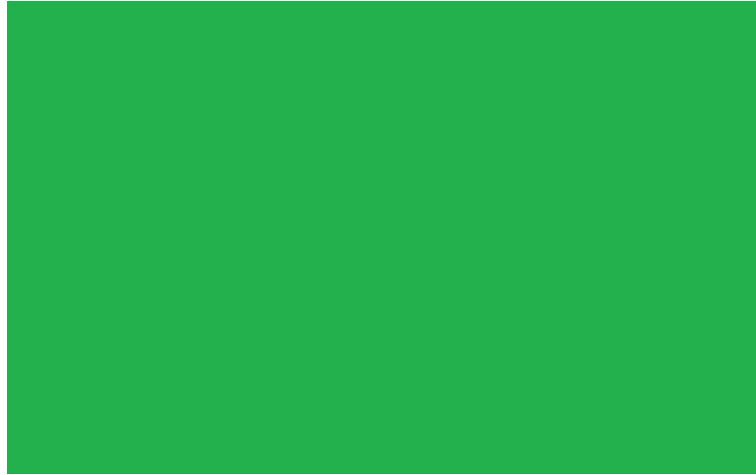

Figure I.12:   dot334 QD150521/22 and dot390 QD14 spectra + dot334 QD150521/22 and dot390 QD14 linear pol + dot334 QD150521/22 magneto-optics

One common feature of all of these dot is the well defined X^c-Cr structures emission, shown on Fig. I.12 (a) between 1946meV (X^--Cr) and 1950mev (X^+-Cr). Such QDs always present thin emission peaks and well splitted X^c-Cr emission peaks. X-Cr and X^2-Cr appear in two different form in σ polarization detection. In Fig. I.12 (a), we can see these two structures appearing with three well defined peaks, with a broad emission. The second type of emission observed is presented in Fig. I.12 (c). One can see the three are here not distinguishable, only a broad emission band is measured at their positions. However, when detecting in π polarization (Fig. I.12 (b) and (d)), both present the same structure: six peaks with linear polarization dependency.

This figure is would be coherent of a QD with a strong E. To analyse them further, magneto-optic experiments were performed on these dots. The result of such an experiment is presented in Fig. I.12 (e). The shift induced by the diamagnetic shift and the Zeeman is clearly visible. However, no anti-crossing appear whatever the magnetic field applied. As shown in I.1.2, QD with a high in-plane anisotropy should present several anti-crossing, especially around 0T. The picture is then not coherent with these low symmetry quantum dots.

Figure I.13: dot390 QD4 electric field map zoom on X+-Cr

In order to have more informations on these dots, it was decided to study them under electric field. In order to apply such an electric field, we realized a sample with the same structure as the one presented in chapter **??**. The resulting map is presented in Fig. I.13. The first visible feature is the strong electric field dependency of the emission, more marked for X-Cr than for the X^c-Cr systems. The emission energy variation of the X-Cr complex occur on a 2.9meV scale.

There is another remarkable point on these maps, evidenced on the two X^+-Cr

complex on the Fig. I.13 (b): the splitting between each peak is changing with the applied electric field. The emission extension vary from 0meV for an applied bias voltage of -12V (no splitting) to 0.76meV for 13V applied.

Figure I.14: dot390 QD14 map under E field (cut at -4V) + spectra at E = -2.5V and E = 0V + linear polar at E = -2.5V and E = 0V

Curabitur eget ipsum egestas dui viverra suscipit. Cras aliquet lacus vitae erat finibus semper. Nulla pharetra eget urna vitae sodales. Nunc faucibus velit lacus, nec ornare eros aliquet quis. Donec a orci nec sem pulvinar ultricies sit amet ut arcu. Nullam id vehicula enim, at tincidunt velit. Duis vestibulum lorem a molestie fringilla. Nullam tincidunt semper placerat. Donec nibh sem, ornare eget cursus ac, luctus sit amet eros. Phasellus eget interdum nisi. Donec mollis risus id lectus fringilla, et commodo risus iaculis. Donec at lacus sed nibh posuere posuere sit amet eget sapien. In dignissim, enim sit amet convallis fermentum, lacus nulla gravida tortor, non facilisis ex nisl sit amet augue. Maecenas eu enim condimentum, consectetur ligula vel, tincidunt nisl. Nam laoreet dictum volutpat. Donec at erat venenatis, ultrices lorem ac, vestibulum neque.

Chapter II

Bibliography

[1] L. Besombes and H. Boukari. Resonant optical pumping of a Mn spin in a strain-free quantum dot. *Phys. Rev. B*, 89:085315, Feb 2014.

[2] T. Takagahara. Theory of exciton doublet structures and polarization relaxation in single quantum dots. *Phys. Rev. B*, 62:16840–16855, Dec 2000.

[3] J. McFarlane, P. A. Dalgarno, B. D. Gerardot, R. H. Hadfield, R. J. Warburton, K. Karrai, A. Badolato, and P. M. Petroff. Gigahertz bandwidth electrical control over a dark exciton-based memory bit in a single quantum dot. *Applied Physics Letters*, 94(9):093113, 2009.

[4] M. Bayer, G. Ortner, O. Stern, A. Kuther, A. A. Gorbunov, A. Forchel, P. Hawrylak, S. Fafard, K. Hinzer, T. L. Reinecke, S. N. Walck, J. P. Reithmaier, F. Klopf, and F. Schäfer. Fine structure of neutral and charged excitons in self-assembled in(ga)as/(al)gaas quantum dots. *Phys. Rev. B*, 65:195315, May 2002.

[5] J. T. Vallin and G. D. Watkins. Epr of cr^{2+} in II-VI lattices. *Phys. Rev. B*, 9:2051–2072, Mar 1974.

[6] W. Mac, A. Twardowski, and M. Demianiuk. s,p-d exchange interaction in Cr-based diluted magnetic semiconductors. *Phys. Rev. B*, 54:5528–5535, Aug 1996.

[7] M. Herbich, W. Mac, A. Twardowski, K. Ando, Y. Shapira, and M. Demianiuk. Magnetization and exciton spectroscopy of the diluted magnetic semiconductor cd$_{1-x}$cr$_x$S. *Phys. Rev. B*, 58:1912–1921, Jul 1998.

[8] D. Gammon, E. S. Snow, B. V. Shanabrook, D. S. Katzer, and D. Park. Fine structure splitting in the optical spectra of single GaAs quantum dots. *Phys. Rev. Lett.*, 76:3005–3008, Apr 1996.

[9] Y. Léger, L. Besombes, L. Maingault, D. Ferrand, and H. Mariette. Geometrical effects on the optical properties of quantum dots doped with a single magnetic atom. *Phys. Rev. Lett.*, 95:047403, Jul 2005.

[10] M. Zieliński, Y. Don, and D. Gershoni. Atomistic theory of dark excitons in self-assembled quantum dots of reduced symmetry. *Phys. Rev. B*, 91:085403, Feb 2015.

[11] L. Besombes, Y. Leger, L. Maingault, D. Ferrand, H. Mariette, and J. Cibert. Carrier-induced spin splitting of an individual magnetic atom embedded in a quantum dot. *Phys. Rev. B*, 71:161307, Apr 2005.

[12] Anna H. Trojnar, Marek Korkusinski, Udson C. Mendes, Mateusz Goryca, Maciej Koperski, Tomasz Smolenski, Piotr Kossacki, Piotr Wojnar, and Pawel Hawrylak. Fine structure of a biexciton in a single quantum dot with a magnetic impurity. *Phys. Rev. B*, 87:205311, May 2013.

[13] B. Varghese, H. Boukari, and L. Besombes. Dynamics of a Mn spin coupled to a single hole confined in a quantum dot. *Phys. Rev. B*, 90:115307, Sep 2014.

[14] Y. Léger, L. Besombes, L. Maingault, and H. Mariette. Valence-band mixing in neutral, charged, and Mn-doped self-assembled quantum dots. *Phys. Rev. B*, 76:045331, Jul 2007.

[15] Michael A. Reshchikov, Anita J. Olsen, Marilyn F. Bishop, and Tom McMullen. Superlinear increase of photoluminescence with excitation intensity in Zn-doped GaN. *Phys. Rev. B*, 88:075204, Aug 2013.